35th Annual International Conference of the IEEE EMBS
Osaka, Japan, 3 - 7 July, 2013

Forward Kinematics Using IMU On-body Sensor Network for Mobile Analysis of Human Kinematics

Thomas Taylor[1], Seungoh Ko[2], Carlos Mastrangelo[3] and Stacy J. Morris Bamberg[4]

***Abstract*— The feasibility of large network inertial measurement units (IMUs) are evaluated for purposes requiring feedback. A series of wireless IMUs were attached to a human lower-limb laboratory model outfitted with joint angle encoders. The goal was to discover if large networks of wireless IMUs can give realtime joint orientation data while still maintaining an acceptable degree of accuracy.**

I. INTRODUCTION

Nearly 10 million, or 5.2%, of U.S. adults between 18-64 years are classified with an ambulatory (walking) disability [1]. Problems in the motor and/or sensory systems can result in impaired ambulation, a disability that is generally associated with a decreased proprioceptive sense, i.e. not knowing where the limbs are or what sensory information the limbs are receiving. In order to observe motion outside the home, devices containing accelerometers, and in some cases gyroscopes and/or magnetometers have been widely used, especially as wearables for older adults [2]–[10]. A remaining challenge is evaluation in real-life settings [11]. The need for augmented feedback to improve mobility has been demonstrated through the use of Lokomat for children with cerebral palsy, an area that demonstrates the need for augmented feedback [12]. A recent review found that most studies of such devices (including commercial) had limited effectiveness, in large part due to required in-clinic use, suggesting future studies should allow feedback "be applied during a prolonged period of time," e.g. at home [13].

The broad appeal and low-cost nature of accelerometers has resulted in many implementations, including commercial packages such as those from Shimmer [14] and Texas Instruments [15]. Units such as these have high appeal for evaluating and providing feedback to patients in the home environment. Other applications could involve sports analysis or even actors in settings where motion analysis cameras are difficult to deploy.

This paper introduces our analysis of multiple units, which each have 3-axis accelerometers, 3-axis gyroscopes, and 3-axis magnetometers, mounted on the same rigid segments. A laboratory model of a lower-limb instrumented with encoders is used for evaluation, with three units on the tibia and three on the foot. The feasibility of large network inertial measurement units (IMUs) for motion capture purposes are evaluated by moving the lower-limb laboratory model randomly and determining if the attached IMUs can adequately capture and send data to a host computer for realtime feedback.

[1]Thomas Taylor is a student of Mechanical Engineering, University of Utah, 72 S. Central Campus Drive, Salt Lake City, UT 84112 `thomas.d.taylor at utah.edu`

[2]Seungoh Ko is a student of Electrical Engineering, University of Utah, 72 S. Central Campus Drive, Salt Lake City, UT 84112 `koseungoh at gmail.com`

[3]Carlos H. Mastrangelo is a USTAR professor of Electrical and Computer Engineering, University of Utah, 72 S. Central Campus Drive, Salt Lake City, UT 84112 `mastrang at eng.utah.edu`

[4]Stacy Bamber is an associate professor of Mechanical Engineering, University of Utah, 72 S. Central Campus Drive, Salt Lake City, UT 84112 `stacy.bamberg at utah.edu`

II. BACKGROUND

Each IMU contains a 3-axis gyroscope, a 3-axis accelerometer, and a 3-axis magnetometer. All orientation measurements are calculated from the 3-axis gyroscope which returns a 16-bit value of the angular velocity of each axis. A direction cosine matrix (DCM) is created to store the absolute orientation of the IMU based on numerical integration of each gyroscope [16]. Gyroscopes have noticeable drift over time and numerical integration can produce significant error over stretches of time; to counteract this, the accelerometer and magnetometer are used to keep the device centered. Each IMU is also equipped with an XBee™wireless module to send periodic transmissions to a host computer for data collection.

Calculation of the IMU's rotation matrix is created with a version of Euler's Method of integration. The initial rotation matrix of the IMU is determined during initialization and each subsequent rotation matrix is determined from [16]:

$$\mathbf{R}(t+dt) = \mathbf{R}(t)\begin{bmatrix} 1 & -d\theta_z & d\theta_y \\ d\theta_z & 1 & -d\theta_x \\ -d\theta_y & d\theta_x & 1 \end{bmatrix} \quad (1)$$

$$d\theta_x = \omega_x dt \quad (2)$$

$$d\theta_y = \omega_y dt \quad (3)$$

$$d\theta_z = \omega_z dt \quad (4)$$

where ω is the angular velocity about each axis and dt is a predetermined time step. Essentially, each new rotation matrix is computed by taking the previous rotation matrix and rotating it by small angles about each axis.

To correct for error, a few techniques are used. Because each axis should remain orthogonal to each other, "renormalization" can be used to enforce this condition [16]. First the X and Y rows of the computed matrix are pulled off in to separate vectors. The dot product of these two axis should be zero because they are orthogonal. This allows a vector error to be determined:

$$error = \mathbf{X} \cdot \mathbf{Y} \quad (5)$$

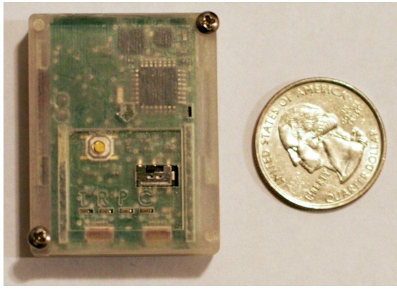

Fig. 1. IMU sensor with attached XBee™wireless transmitter.

This error is then appropriated between the two axis by half and the Z axis is found using the cross product:

$$\mathbf{X}_{orthogonal} = \mathbf{X} - \frac{error}{2}\mathbf{Y} \quad (6)$$
$$\mathbf{Y}_{orthogonal} = \mathbf{Y} - \frac{error}{2}\mathbf{X} \quad (7)$$
$$\mathbf{Z}_{orthogonal} = \mathbf{X}_{orthogonal} \times \mathbf{Y}_{orthogonal} \quad (8)$$

The final step is to renormalize the vectors to assure that the magnitude of each vector is one. To decrease computation time, a Taylor's expansion can be done resulting in [16]:

$$\mathbf{X}_{normalized} = \frac{1}{2}(3 - \mathbf{X}_{orth} \cdot \mathbf{X}_{orth})\mathbf{X}_{orth} \quad (9)$$
$$\mathbf{Y}_{normalized} = \frac{1}{2}(3 - \mathbf{Y}_{orth} \cdot \mathbf{Y}_{orth})\mathbf{Y}_{orth} \quad (10)$$
$$\mathbf{Z}_{normalized} = \frac{1}{2}(3 - \mathbf{Z}_{orth} \cdot \mathbf{Z}_{orth})\mathbf{Z}_{orth} \quad (11)$$

These steps can produce accurate results for the direction cosine matrix from the gyroscope readings. The previously mentioned drift problems that come from using numerical integration and gyroscopes prevent completely accurate results. To correct for this, the accelerometer and magnetometer are used to zero the gyroscopes. The accelerometer and magnetometer can each give an axis that does not drift that can be used as a reference. For this particular setup, the accelerometer was used for the X and Y axis and the magnetometer was used to correct for rotations about Z. To fix the drift, a simple PI controller feedback loop was used. This allowed the corrections to be tuned such that the drift cancelation was fast and accurate.

III. Methods

To test the accuracy of both individual and redundant IMUs, a mechanical leg approximating motion of a human leg was built. This leg consists of a 3-DOF joint to simulate the joint connection to the hip, a 1-DOF knee joint, and a 2-DOF ankle joint. The mechanical leg's femur bone consists of a rigid, adjustable, telescoping aluminum rod to use the skeleton for different body sizes. Likewise, the mechanical leg's tibia bone is made from the same telescoping rod. The design of the leg allows for quick adjustment to accommodate different anthropometry values that may be of interest. Each joint has an attached magnetic encoder that returns a 10-bit analog signal. Accuracy of the magnetic encoders are approximately 0.35 degrees when operated at room temperature. For this paper, the femur bone was grounded horizontal to the floor and only the motion of the tibia and foot were analyzed. This decision was made to decrease complexity and focus on the accuracy of the IMUs instead of the forward kinematics of the leg itself.

To test the accuracy of each IMU (Fig. 1) as well as the benefit of multiple IMUs, three IMUs were attached to both the tibia and the foot. The IMUs were mounted with the IMU aligned with the bone (from knee to ankle and then from ankle to toe) while the IMU's normal vector pointed toward the ground if the leg and foot were to be extended out horizontally. Each IMU was programmed to send out information packets (consisting of roll, pitch, and yaw Euler angles as well as a time stamp synchronized across IMUs) only when the sensor saw a degree change greater than one-half. This allows the IMUs to be more energy efficient and sleep when not in use. In order to ensure efficient delivery of the data, data was transmitted as two-byte numbers for each angle and a four-byte number for the elapsed time in milliseconds. By using bytes for the angle data, resolution is lost to conserve space, but this resolution is still finer than the half a degree change needed to wake the IMU from sleep so no data is lost.

After data collection, the host computer steps through the data and linearly interpolates each sensor so that there is data from each IMU at every time step. Because of the sleep-interrupt-wake feature employed in the IMUs to preserve battery life, data does not come in at predictable intervals. By doing a sensor by sensor linear interpolation, this problem is addressed. In a separate process, another program gathered readings from the artificial leg's joint encoders, again with an attached time stamp.

The data collection process is as follows:

1) Turn on each sensor and zero all accelerometer and gyroscope readings.
2) Connect each sensor to the host computer and place each sensor in stasis.
3) Attach each sensor to the artificial leg in the orientation heretofore mentioned.
4) Start data collection for the leg's encoders.
5) Ping each sensor to synchronize clocks and start sending data.
6) Randomly move the joints of the leg for about twenty seconds.
7) Linearize the IMU data.
8) Apply calibration to magnetometer

The magnetometer works much like a compass. It has an internal spindle that aligns itself with the nearest magnetic field and it is hoped that this magnetic field is pointing toward Magnetic North. If there are small local magnetic fields which can be present from running electronic equipment in the room or even the room's structural material, the magnetometers can produce an incorrect alignment. To make matters worse, each magnetometer for each IMU does not have a factory calibration done by the manufacturer so a batch of magnetometers can behave differently.

To overcome this obstacle of misaligned magnetometer headings, the IMUs can be centered locally by knowing the

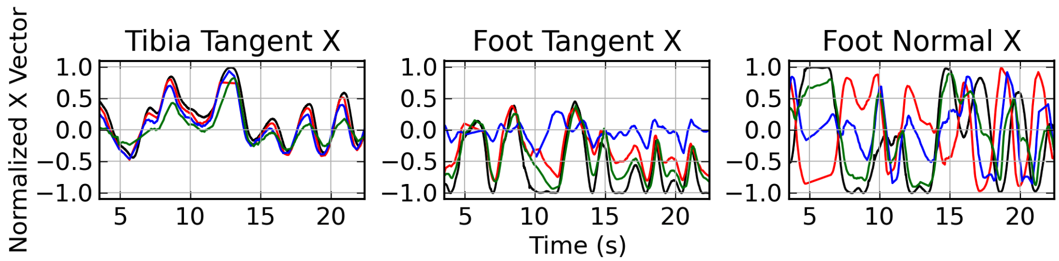

Fig. 2. Raw x component data for vectors calculated from the IMU. Note that although there are only 3 sensors per joint (Tibia and Foot), the foot has enough degrees of freedom to require both a vector that is tangent to the foot and a vector normal to the foot to be calculated. The black curve represents the true vector heading and the red, green, and blue curves represents output from the three sensors per joint.

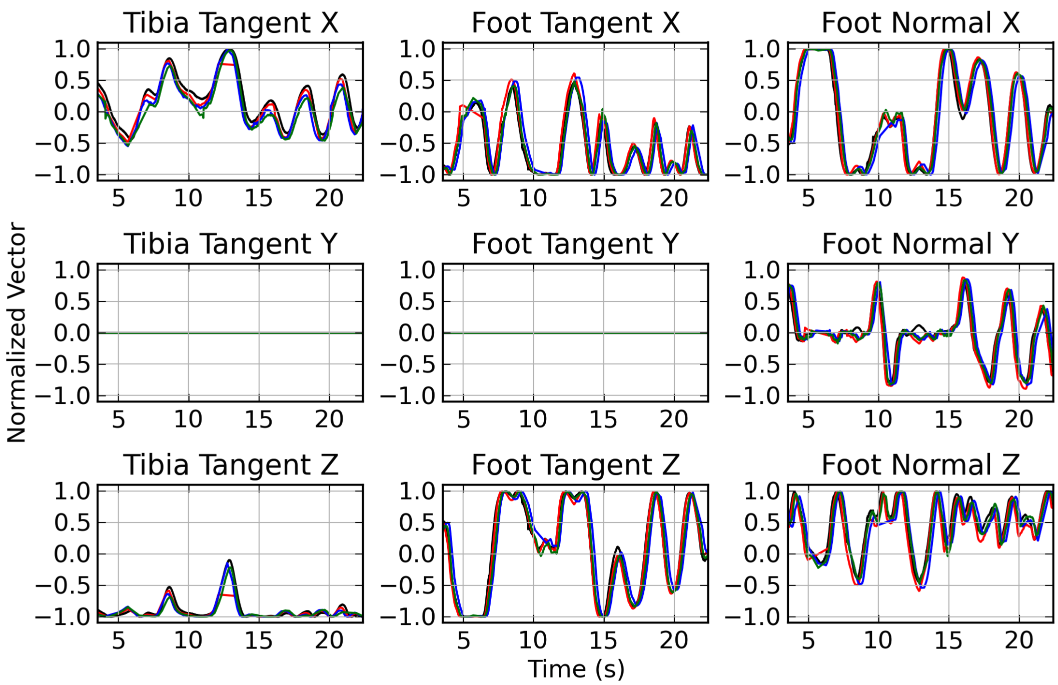

Fig. 3. Output from calibrated sensors. Three sensors are attached to each joint and full x, y, and z components of the calculated vectors are shown. The foot joint has enough degrees of freedom that two vectors (a tangent and normal) are needed. The black curves represent the true values of each joint and the red, green, and blue curves represent outputs from the sensors.

true heading of the body the IMU is attached to. Much like a scale can be calibrated by weighing a mass of known value, the IMUs can be post calibrated by knowing the true tangential vector heading. The leg was positioned so that it points toward Magnetic North which means the tangential vector of the IMU must lie in the X-Z plane. By finding the angle the magnetometer has shifted from this heading, the IMU can be rotated back to the correct heading.

The first step is to find out how far out of alignment the IMU is oriented. To do this, the X and Y components of the heading vector are considered. By finding the tangent of the two components, the angle deviation from the X-axis can be determined. Note that the graphical quadrant the resultant vector is located in is very important; a resultant vector in quadrant II for instance must be rotated *counter-clockwise* to be in alignment with the X-axis. The tangent function has a reduced range because $\tan(\frac{y}{x})$ yields the same result as $\tan(\frac{-y}{-x})$. This shortcoming is resolved by using the *ATAN2* function present in most programming language math libraries. This function expands the range of the tangent function to $[-\pi, \pi]$ with the knowledge of what the signs of x and y are.

After the quadrant is determined, the sensor can be re-calibrated and pulled back to the X-axis. This is done with a two-dimensional vector rotation:

$$x' = x \cos\theta - y \sin\theta \quad (12)$$

$$y' = x \sin\theta + y \cos\theta \quad (13)$$

where θ is the rotation of the vector in a counter-clockwise direction, x and y are the original vector components and x' and y' are the components of the new rotated vector. The rotation logic then becomes:

- If in Quadrant I, rotate the vector by $-\theta$
- If in Quadrant II, rotate the vector by $\pi - \theta$
- If in Quadrant III, rotate the vector by $-\pi - \theta$

- If in Quadrant IV, rotate the vector by $-\theta$

The normal vector of the foot is a little more complicated to correct because there is not a single axis to correct against. The two compounded ankle rotations allows the normal vector to move in all three axis. To correct for this vector, first the IMU is correctly oriented along the axis of the foot. Secondly, the forward vector is rotated $-\frac{\pi}{2}$ about the IMU's Y-axis. This new vector is the IMU's normal vector. Finally, this normal vector is rotated about the IMU's tangential axis by the value of *roll* - one of the three Euler Angles - which is output from the sensor.

$$up'_y = up_y \cos roll - up_z \sin roll \quad (14)$$

$$up'_z = up_y \sin roll + up_z \cos roll \quad (15)$$

IV. Results

Results from the raw data are shown in Fig. 2. Each plot shows the x-component of either the tangent or normal vector of each IMU as well as where the true heading of this component should be as calculated from the artificial leg's encoders. Error from the IMU magnetometers are visible in each plot with particular noise found in the IMUs mounted to the foot. Fig. 3 shows the data after being calibrated using the *ATAN2* method.

V. Discussion

Fig. 3 shows data that is significantly corrected from the raw IMU data. Instead of the noisy data seen in Fig. 2, data is consistent across IMUs and matches the expected values calculated from the artificial leg. Some errors are still present, for instance in *Tibia Tangent X* and *Tibia Tangent Z*, one of the IMUs cuts across a "hump" around the 12 second mark. This occurs because this particular sensor did not send out data for a brief period of time. Because all of the IMU data is linearized to provide an orientation point for all IMUs for all time, if there is a break in data, the true curve can not be correctly determined.

Also, the *Foot Normal Y* plot shows incorrect calculation at about 9 minutes and 13 seconds. Closer examination shows that the computed magnitude of the incorrect "humps" is what is expected, but the sign of the data has been flipped. When this happens, it is an indication that there is a range error corresponding to the $\cos$ and $\sin$ functions used for data analysis. Because these functions operate on a circle, it is possible for an angle to move out of bounds temporarily and produce error. More analysis is necessary to ensure that small errors like this are no longer existent.

The IMUs are sufficient to be used in real time networked applications as shown. For future work, the aforementioned calculation errors need to be resolved and larger networks of IMUs should be tested. If very large networks of IMUs are shown to be effaceable, very accurate real time motion capture data is possible without a dedicated lab. Effort should be made to apply averaging methods to the IMUs to try and arrive at more accurate and reliable information. Planned future work consists of refining a Kalman filter that would allow the user to trust data if it has arrived with certain criteria such as data that is closer to nearby IMUs or to trust data more if it comes from an IMU that pings the host computer frequently.

The method in this paper has shown that it is possible to get reasonably accurate information from IMUs and that it is possible to scale the number of IMUs present on a body and still achieve real time results. Greater networks of IMUs will need to be tried so that lower cost motion capture systems can be available outside of dedicated laboratories.

References

[1] R. Research, T. C. on Disability Statistics, and Demographics, "Annual disability statistics compendium," 2010.

[2] S. Patel, K. Lorincz, R. Hughes, N. Huggins, J. Growdon, D. Standaert, M. Akay, J. Dy, M. Welsh, and P. Bonato, "Monitoring motor fluctuations in patients with parkinson's disease using wearable sensors," in *IEEE Transactions On Information Technology in Biomedicine*, vol. 13, November 2009, pp. 864–873.

[3] T.-T. Nguyen, M.-C. Cho, and T.-S. Lee, "Automatic fall detection using wearable biomedical signal measurement terminal," in *31st Annual International Conference of the IEEE EMBS*. IEEE, September 2009, pp. 5203–5206.

[4] M. Kishimoto, T. Yoshida, T. Hayasaka, D. Mori, Y. Imai, N. Matsuki, T. Ishikawa, and T. Yamaguchi, "An internet-based wearable watch-over system for elderly and disabled utilizing emg and accelerometer," in *Technol Health Care*, vol. 17, 2009, pp. 121–131.

[5] M. Hanlon and R. Anderson, "Real-time gait event detection using wearable sensors," in *Gait Posture*, vol. 30, November 2009, pp. 523–527.

[6] W. S. Yeoh, I. Pek, Y. H. Yong, X. Chen, and A. B. Waluyo, "Ambulatory monitoring of human posture and walking speed using wearable accelerometer sensors," in *Conf Proc IEEE Eng Med Biol Soc*, 2008, pp. 5184–5187.

[7] M. V. Wieringen and J. Eklund, "Real-time signal processing of accelerometer data for wearable medical patient monitoring devices," in *Conf Proc IEEE Eng Med Biol Soc*, 2008, pp. 2397–2400.

[8] M. N. Nyan, F. E. Tay, and E. Murugasu, "A wearable system for pre-impact fall detection," in *J Biomech*, vol. 41, December 2008, pp. 3475–3481.

[9] P. Bonato, D. M. Sherrill, D. G. Standaert, S. S. Salles, and M. Akay, "Data mining techniques to detect motor fluctuations in parkinson's disease," in *Conf Proc IEEE Eng Med Biol Soc*, vol. 7, 2004, pp. 4766–4769.

[10] B. R. Chen, S. Patel, T. Buckley, R. Rednic, D. J. McClure, L. Shih, D. Tarsy, M. Welsh, and P. Bonato, "A web-based system for home monitoring of patients with parkinson's disease using wearable sensors," in *IEEE Trans Biomed Eng*, vol. 58, March 2010, pp. 831–836.

[11] E. D. de Bruin, A. Hartmann, D. Uebelhart, K. Murer, and W. Zijlstra, "Wearable systems for monitoring mobility-related activities in older people: a systematic review," in *Clin Rehabil*, vol. 22, October 2008, pp. 878–895.

[12] B. Patritti, M. Sicari, L. Deming, F. Romaguera, M. Pelliccio, M. G. Benedetti, D. Nimec, and P. Bonato, "Enhancing robotic gait training via augmented feedback," in *Engineering in Medicine and Biology Society (EMBC), 2010 Annual International Conference of the IEEE*, 2010, pp. 2271–2274.

[13] A. Zijlstra, M. Mancini, L. Chiari, and W. Zijlstra, "Biofeedback for training balance and mobility tasks in older populations: a systematic review," in *J Neuroeng Rehabil*, vol. 7, 2010, p. 15.

[14] S. Research. [Online]. Available: http://www.shimmer-research.com/

[15] [Online]. Available: http://www.ti.com/tool/cc2541dk-sensor?DCMP=blestackHQS=blestack13-pr-tf1buy

[16] W. Premerlani and P. Bizard, "Direction cosine matrix imu: Theory," May 2009, http://gentlenav.googlecode.com/files/MahonyPapers.zip.